

# Coexistence and interaction of vector and bound vector solitons in a dispersion-managed fiber laser mode locked by graphene

Y. F. Song,<sup>1</sup> H. Zhang,<sup>1,4</sup> L. M. Zhao,<sup>3</sup> D. Y. Shen,<sup>3</sup> and D. Y. Tang,<sup>2,5</sup>

<sup>1</sup>*SZU-NUS Collaborative Innovation Center for Optoelectronic Science & Technology, Key Laboratory of Optoelectronic Devices and Systems of Ministry of Education and Guangdong Province, College of Optoelectronic Engineering, Shenzhen University, Shenzhen 518060, China*

<sup>2</sup>*School of Electrical and Electronic Engineering, Nanyang Technological University, 639798, Singapore*

<sup>3</sup>*Jiangsu Key Laboratory of Laser Materials and Devices, School of Physics and Electronic Engineering, Jiangsu Normal University, 221116, China*

<sup>4</sup>[hzhang@szu.edu.cn](mailto:hzhang@szu.edu.cn)

<sup>5</sup>[edytang@ntu.edu.sg](mailto:edytang@ntu.edu.sg)

**Abstract:** We report on the experimental observation of vector and bound vector solitons in a fiber laser passively mode locked by graphene. Localized interactions between vector solitons, vector soliton with bound vector solitons, and vector soliton with a bunch of vector solitons are experimentally investigated. We show that depending on the soliton interactions, various stable and dynamic multiple vector soliton states could be formed.

©2016 Optical Society of America

**OCIS codes:** (060.4370) Nonlinear optics, fibers; (060.5530) Pulse propagation and temporal solitons.

---

## References and links

1. B. A. Malomed, "Bound solitons in the nonlinear Schrödinger-Ginzburg-Landau equation," *Phys. Rev. A* **44**(10), 6954–6957 (1991).
2. B. A. Malomed, "Bound solitons in coupled nonlinear Schrödinger equations," *Phys. Rev. A* **45**(12), R8321–R8323 (1992).
3. N. N. Akhmediev, A. Ankiewicz, and J. Soto-Crespo, "Multisoliton solutions of the complex Ginzburg-Landau equation," *Phys. Rev. Lett.* **79**(21), 4047–4051 (1997).
4. N. N. Akhmediev, A. Ankiewicz, and J. M. Soto-Crespo, "Stable soliton pairs in optical transmission lines and fiber lasers," *J. Opt. Soc. Am. B* **15**(2), 515–523 (1998).
5. S. Latas and M. Ferreira, "Bound States of dissipative solitons in optical fiber systems," in *Proceedings of the SPIE - The International Society for Optical Engineering*, 7582, p 75820P (9 pp.), 2010.
6. P. Grelu and N. Akhmediev, "Dissipative solitons for mode locked lasers," *Nat. Photonics* **6**(2), 84–92 (2012).
7. D. Y. Tang, W. S. Man, H. Y. Tam, and P. D. Drummond, "Observation of bound states of solitons in a passively mode-locked fiber laser," *Phys. Rev. A* **64**(3), 033814 (2001).
8. L. Gui, X. Xiao, and C. Yang, "Observation of various bound solitons in a carbon-nanotube-based erbium fiber laser," *J. Opt. Soc. Am. B* **30**(1), 158–164 (2013).
9. X. Wu, D. Tang, X. N. Luan, and Q. Zhang, "Bound states of solitons in a fiber laser mode locked with carbon nanotube saturable absorber," *Opt. Commun.* **284**(14), 3615–3618 (2011).
10. C. Zeng, Y. D. Cui, and J. Guo, "Observation of dual-wavelength solitons and bound states in a nanotube/microfiber mode-locking fiber laser," *Opt. Commun.* **347**, 44–49 (2015).
11. C. Mou, S. V. Sergeyev, A. G. Rozhin, and S. K. Turitsyn, "Bound state vector solitons with locked and precessing states of polarization," *Opt. Express* **21**(22), 26868–26875 (2013).
12. H. H. Liu and K. K. Chow, "High fundamental-repetition-rate bound solitons in carbon nanotube-based fiber lasers," *IEEE Photonics Technol. Lett.* **27**(8), 867–870 (2015).
13. H. R. Yang, G. W. Chen, Y. C. Kong, and W. L. Li, "Bound-state fiber laser mode-locked by a graphene-nanotube saturable absorber," *Laser Phys.* **25**(2), 025101 (2015).
14. X. Li, S. Zhang, Y. Meng, Y. Hao, H. Li, J. Du, and Z. Yang, "Observation of soliton bound states in a graphene mode locked erbium-doped fiber laser," *Laser Phys.* **22**(4), 774–777 (2012).
15. L. Gui, X. Li, X. Xiao, H. Zhu, and C. Yang, "Widely spaced bound states in a soliton fiber laser with graphene saturable absorber," *IEEE Photonics Technol. Lett.* **25**(12), 1184–1187 (2013).
16. Y. Wang, D. Mao, X. Gan, L. Han, C. Ma, T. Xi, Y. Zhang, W. Shang, S. Hua, and J. Zhao, "Harmonic mode locking of bound-state solitons fiber laser based on MoS<sub>2</sub> saturable absorber," *Opt. Express* **23**(1), 205–210 (2015).

17. J. W. Haus, G. Shaulov, E. A. Kuzin, and J. Sanchez-Mondragon, "Vector soliton fiber lasers," *Opt. Lett.* **24**(6), 376–378 (1999).
18. B. C. Collings, S. T. Cundiff, N. N. Akhmediev, J. M. Soto-Crespo, K. Bergman, and W. H. Knox, "Polarization-locked temporal vector solitons in a fiber laser: experiment," *J. Opt. Soc. Am. B* **17**(3), 354–365 (2000).
19. D. Y. Tang, B. Zhao, L. M. Zhao, and H. Y. Tam, "Soliton interaction in a fiber ring laser," *Phys. Rev. E Stat. Nonlin. Soft Matter Phys.* **72**(1), 016616 (2005).
20. A. Reina, X. Jia, J. Ho, D. Nezich, H. Son, V. Bulovic, M. S. Dresselhaus, and J. Kong, "Large area, few-layer graphene films on arbitrary substrates by chemical vapor deposition," *Nano Lett.* **9**(1), 30–35 (2009).
21. S. M. Kelly, "Characteristic sideband instability of periodically amplified average soliton," *Electron. Lett.* **28**(8), 806–807 (1992).
22. P. Grelu, F. Belhache, F. Guty, and J. M. Soto-Crespo, "Phase-locked soliton pairs in a stretched-pulse fiber laser," *Opt. Lett.* **27**(11), 966–968 (2002).
23. V. Besse, H. Leblond, D. Mihalache, and B. A. Malomed, "Pattern formation by kicked solitons in the two-dimensional Ginzburg-Landau medium with a transverse grating," *Phys. Rev. E Stat. Nonlin. Soft Matter Phys.* **87**(1), 012916 (2013).
24. V. Besse, H. Leblond, D. Mihalache, and B. A. Malomed, "Building patterns by traveling dipoles and vortices in two-dimensional periodic dissipative media," *Opt. Commun.* **332**, 279–291 (2014).

## 1. Introduction

Bound states of solitons, also known as soliton molecules, are referred to that two or more fundamental solitons bind tightly together in the temporal or spatial domain through the direct soliton interaction. The solitons in the state have not only fixed separations but also fixed phase differences, and the assembly of the solitons behaves like a new super-soliton. Theoretically, formation of bound states of solitons in the extended nonlinear Schrödinger equation (NLSE) systems was first predicted by B. Malomed [1, 2]. N. N. Akhmediev *et al.* had also studied the formation of bound states of solitons in the complex Ginzburg-Landau equation (CGLE) systems [3, 4]. It was shown that dissipative property renders the solitons with unique new features of interaction that can result in the formation of stable bound states of dissipative solitons [5].

Experimentally, formation of bound states of solitons in fiber lasers has attracted considerable interest. Owing to the existence of gain and losses, solitons formed in a fiber laser are essentially dissipative solitons [6]. It is anticipated that the soliton fiber lasers could serve as an ideal testbed for the study on bound solitons. The bound states of solitons were first experimentally observed in a fiber laser mode locked with the nonlinear polarization rotation (NPR) technique [7]. Later, with the development of novel material based real saturable absorber (SA) mode locking techniques, such as the carbon nanotube mode locking, 2D-nano-materials mode locking, formation of bound states of solitons has also been observed in fiber lasers mode locked with the carbon nanotubes [8–12], graphene [13–15] and MoS<sub>2</sub> [16]. Unlike the NPR mode-locked fiber lasers where the formed solitons have a fixed polarization due to the insertion of a polarizer in cavity, the polarization insensitive saturable absorption of the carbon nanotube and graphene saturable absorbers allows the formation of vector solitons in fiber lasers. Here a vector soliton is referred to as a soliton that has two coupled orthogonal polarization components [17]. Therefore, one would expect that bound states of dissipative vector solitons could also be formed in fiber lasers mode locked with these saturable absorbers. We note that the phase locked vector solitons were first experimentally observed in a SESAM mode locked fiber laser [18]. C. Mou *et al.* reported the existence of bound vector solitons in a carbon nanotube mode locked fiber laser [11]. However, so far the experimental studies have mainly focused on the formation of the bound solitons or bound vector solitons in fiber lasers. Although it is well-known that the formation of bound states of solitons is a result of the direct soliton interaction [1, 7, 19], how the bound solitons interact or a soliton interacts with the bound solitons has not been addressed.

In this paper we report on the experimental study of interaction between the vector solitons and bound vector solitons in a fiber laser passively mode locked with graphene. In our fiber laser we have obtained various types of solitons, including the vector solitons, bound states of vector solitons, and bound states of bound vector solitons. Coexistence of vector solitons and bound vector solitons in the same laser cavity is also first experimentally

observed. Dispersive wave mediated vector soliton interaction and collision between the vector solitons are also experimentally visualized. Our experimental results confirm the stability and robustness of the bound vector solitons in fiber lasers.

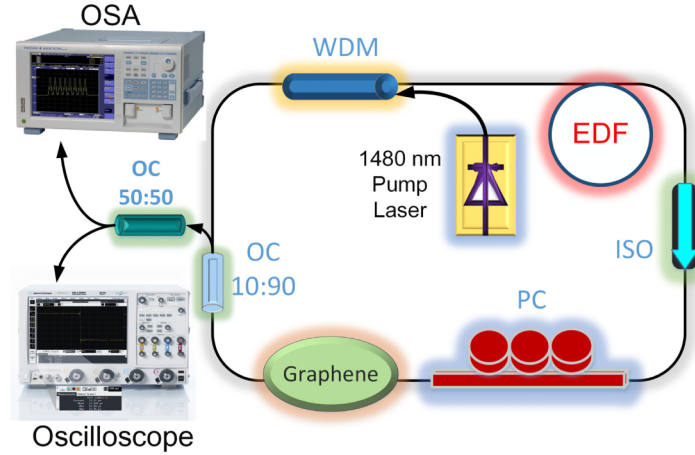


Fig. 1. A schematic diagram of the fiber laser setup. SMF: Single-mode fiber, PC: Polarization controller, EDF: Erbium doped fiber, WDM: Wavelength-division multiplexer, OC: Optical coupler, ISO: Isolator, OSA: Optical spectrum analyser.

## 2. Experimental setup

A schematic of the graphene mode-locked fiber laser is shown in Fig. 1. The fiber laser has a ring cavity of 15.6 m long. A piece of 3 m erbium doped fiber with a group velocity dispersion (GVD) parameter of  $-48$  ps/nm/km was used as the gain fiber. Other fibers used are all the standard single mode fiber (SMF-28) with a GVD parameter of 18 ps/nm/km. Thus the cavity is dispersion-managed and has net anomalous dispersion. A polarization independent isolator is employed in the cavity to force the unidirectional operation of the ring cavity, and an intra-cavity polarization controller (PC) is used to fine-tune the linear cavity birefringence. The laser is reverse pumped by a high power fiber Raman Laser source (KPS-BT2-RFL-1480-60-FA) of wavelength 1480 nm. The pump laser can deliver a maximum pump power as high as 5 W. A 10% output coupler is used to output the laser emission. The graphene used is synthesized using the chemical vapor deposition (CVD) method, and it has multiple layers [20]. The graphene sheets are carefully deposited on the end facet of an optical fiber, which is inserted in a fiber connector. The laser emission is measured by an optical spectrum analyzer (OSA) and a 32 GHz real-time oscilloscope (RTO). The laser output is split into two paths: one is monitored by the OSA and the other by the RTO. Therefore, both the optical spectrum and the time evolution of the laser emission are measured simultaneously. To detect the vector soliton feature of the laser emission, a polarization beam splitter was used to separate the two orthogonal polarizations. In addition, a commercial autocorrelator (FR-103XL) is used to measure the pulse width and observe the details of the bound solitons.

## 3. Experimental results

### 3.1 Vector soliton mode-locking

Mode locking of the fiber laser can self-start at a pump power of  $\sim 100$  mW. Figure 2 illustrates a typical soliton mode locked state of the laser. Figure 2(a) shows the oscilloscope traces of the polarization resolved laser emissions. Along the two orthogonal polarization directions of the laser cavity synchronized pulses are measured. Figure 2(b) shows the corresponding optical spectrum. The 3-dB spectral bandwidth of the laser emission is  $\sim 10.2$

nm. As the fiber laser has a dispersion-managed cavity with a small net anomalous dispersion, the spectral profile displays a near Gaussian shape. Nevertheless, a weak asymmetrical Kelly spectral sideband can still be identified at  $\sim 1571$  nm, which shows that the mode locked pulses have been shaped into dissipative solitons in the fiber laser [21]. It is noted that the number of the soliton pulses in the cavity can be increased or decreased by carefully changing the pump power. The vector nature of the solitons is also confirmed by the coexistence of two synchronized polarization components. Figure 2(c) shows the autocorrelation trace of the solitons. If a  $\text{sech}^2$  profile is assumed, the solitons have a FWHM pulse width of 390 fs, given a time-bandwidth product of 0.492. Therefore, the formed solitons are slightly chirped.

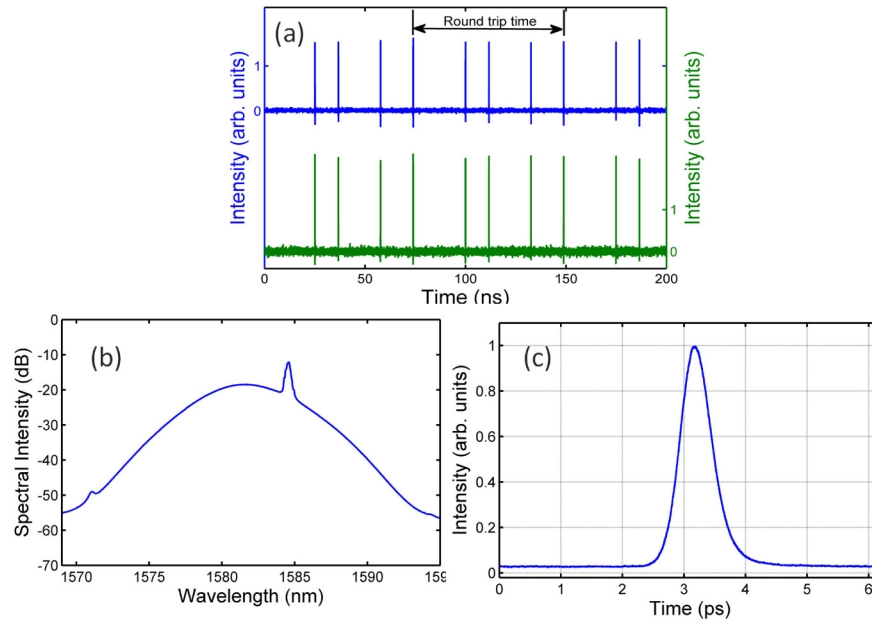


Fig. 2. A typical state of vector soliton operation of the mode locked fiber laser. (a) Oscilloscope trace; (b) Optical spectrum; (c) Autocorrelation trace.

### 3.2 Bound states of vector solitons

Apart from the above multiple vector soliton operation, bound states of vector solitons could also be experimentally observed in the fiber laser. A typical bound state of two vector solitons is shown in Fig. 3. One of the characteristics of the bound solitons is that its optical spectrum is strongly periodically modulated, which reflects the fixed soliton separation [7]. Figure 3(a) shows the total and the polarization resolved optical spectra of the laser emission. As can be seen in Fig. 3(a), the optical spectra of the state are strongly modulated. The spectral modulation period is about 1 nm, which corresponds to a soliton separation of  $\sim 8$  ps in the time domain. The 3-dB spectral bandwidth of the pulses is  $\sim 10.2$  nm, which is the same as that of the fundamental soliton. We note that two CW components also exist in one of the two orthogonal polarization directions. Moreover, the spectral bandwidth of the solitons along the two orthogonal polarization directions, as well as the spectral modulation period and the central wavelength are the same, indicating that the solitons along the two orthogonal polarizations have the same pulse duration and pulse separation. Hence, it is a bound state of vector solitons. The bound state of vector solitons is further confirmed by measuring the autocorrelation trace, as shown in Fig. 3(b). There are three peaks in the trace with a height ratio of 1:2:1, which corresponds to the case where two pulses with identical intensity and duration are bound in the time domain. The measured soliton separation in the bound state is 8.1 ps, which coincides with the modulation period observed on the optical spectrum. The

oscilloscope trace of the bound state of vector solitons is shown in Fig. 3(c). The pulse trace is almost similar to those shown in Fig. 2(b). Due to the limited bandwidth of the oscilloscope, it cannot be determined simply from the oscilloscope traces if the pulse is single soliton or bound solitons.

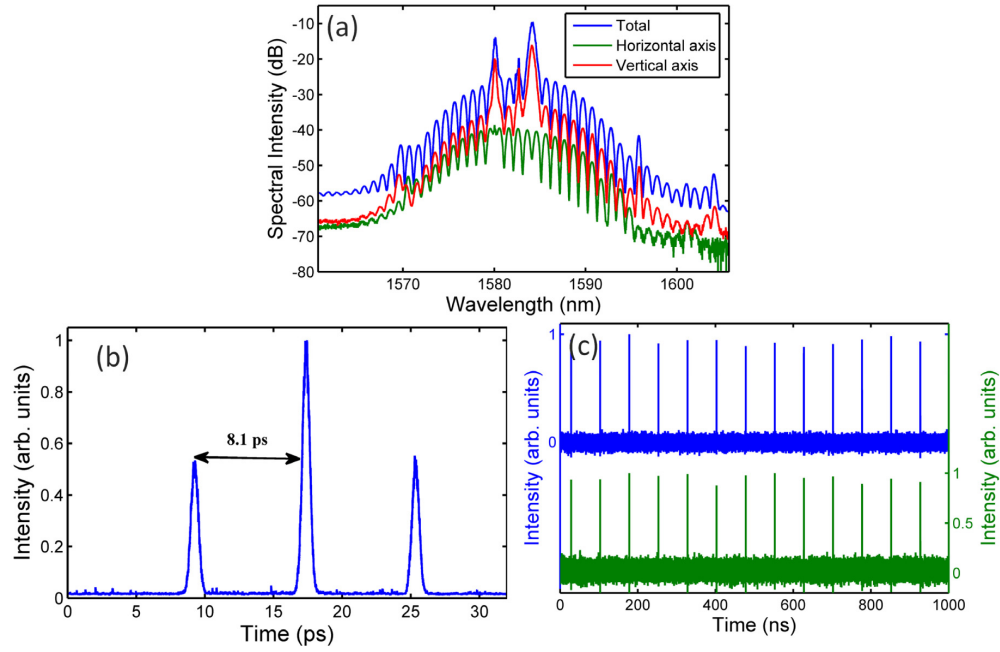


Fig. 3. A state of bound vector solitons of the fiber laser. (a) Optical spectra. Blue line: the total output; Green line: output along the horizontal axis; Red line: output along the vertical axis. (b) Autocorrelation trace; (c) the polarization resolved oscilloscope traces.

### 3.3 Coexistence of vector solitons and bound-vector-solitons

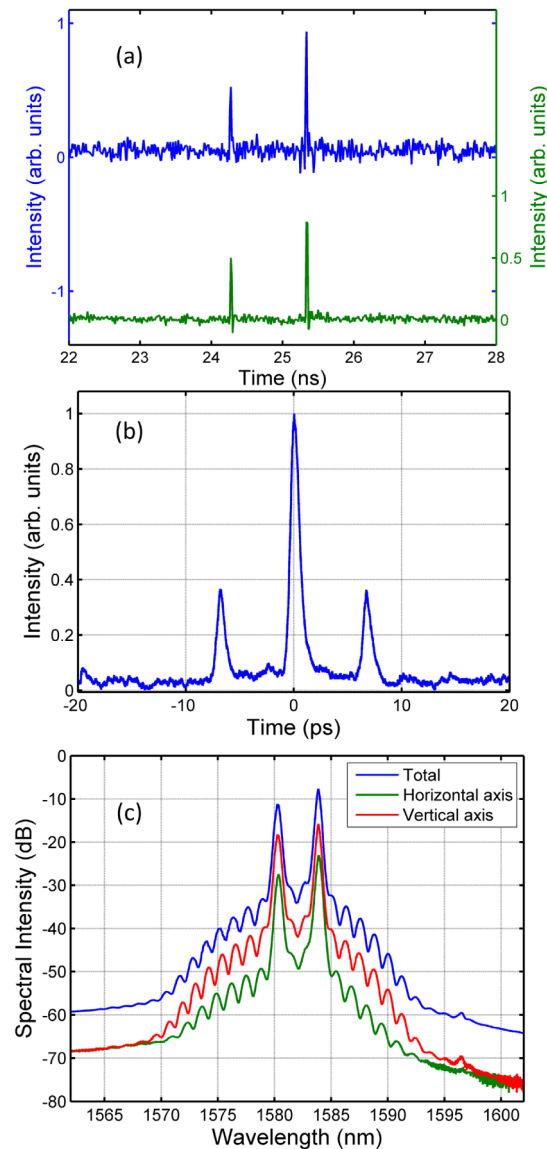


Fig. 4. Coexistence of single soliton and bound solitons. (a) the polarization resolved oscilloscope trace; (b) Autocorrelation trace; (c) Optical spectra.

An interesting soliton operation state of the fiber laser is the coexistence of bound vector solitons and single vector soliton, as shown in Fig. 4. To the best of our knowledge, such a state has never been reported before. The oscilloscope traces in Fig. 4(a) show that two soliton pulses with different pulse intensities coexist in the cavity. The one with higher intensity is a state of bound vector solitons, and the one with lower intensity is a vector soliton. To confirm that the higher intensity one is a bound state of vector solitons, we further measured the autocorrelation trace of the state, it is depicted in Fig. 4(b). Obviously, a bound state of solitons is formed in the laser. However, unlike the autocorrelation trace of the bound solitons shown in Fig. 3(b), where the central peak to the side-peak height ratio is 2:1, in the current case the central peak to the side-peak height ratio is  $\sim 2.5:1$ . The difference is caused

due to the coexistence of the vector soliton in the cavity. The measured autocorrelation trace is actually an average of that of the vector soliton and the bound vector solitons. Considering that the autocorrelation trace of the vector soliton has only one peak (see Fig. 2), one will be able to understand why the intensity ratio of the central peak to side-peak measured in the autocorrelation trace is larger than 2:1. Figure 4(c) shows the corresponding polarization resolved optical spectra. The spectral modulation again confirms the existence of the bound state of vector solitons in the cavity. A spectral dip is at the centre of the spectra, indicating that the bound solitons could have  $\pi$  phase difference [22].

### 3.4 Interaction between vector soliton and bound vector solitons

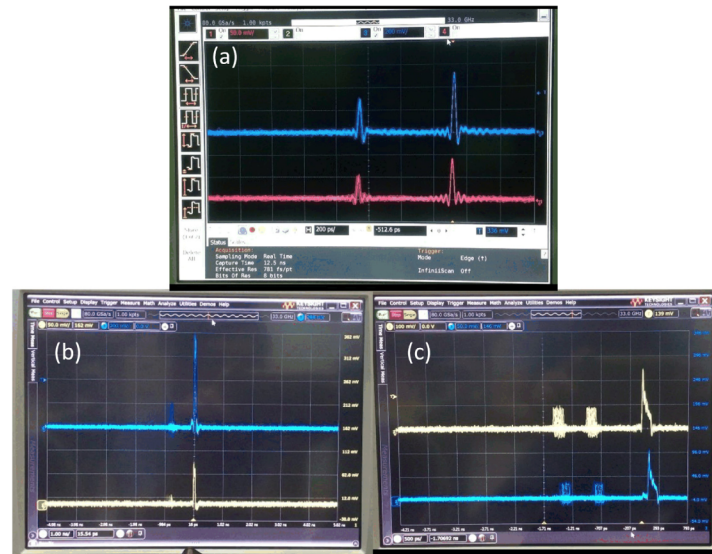


Fig. 5. Interactions between vector soliton and bound vector solitons. (a) Snapshot of the moving solitons and the bound solitons (200 ps/div, see Visualization 1). (b) Snapshot of vector soliton move through a bound vector solitons (1 ns/div, see Visualization 2). (c) Snapshot of vector solitons moving into a soliton bunch (500 ps/div, see Visualization 3).

We have experimentally investigated the interaction between the single vector soliton and the bound vector solitons in the laser cavity. An interesting case is recorded in Visualization 1 of Fig. 5(a). In the case a vector soliton and a bound state of two vector solitons coexist in the cavity. On the oscilloscope traces the pulse with higher intensity is the bound vector solitons while the one with lower intensity is the single vector soliton. As the bound vector solitons are used to trigger the oscilloscope, hence it is stationary in the oscilloscope trace. One can clearly see that the single soliton moves slowly with respect to the bound solitons. However, it is trapped in a certain range and moves repeatedly towards and then away from the bound solitons. The minimum distance that the single soliton comes close to the bound solitons is  $\sim 150$  ps. The soliton interaction is localized. We believe it could be caused by the dispersive waves mediated soliton interaction [19]. Visualization 1 not only provides a direct evidence of the coexistence of the single and the bound vector solitons, but also reveals that they can interact with each other in the laser cavity. By carefully changing the cavity condition, the single and the bound vector solitons can also collide in the cavity. Figure 5(b) (see Visualization 2) shows that a single vector soliton passes through bound vector solitons. It can be clearly seen that the speed of the soliton is significantly reduced after passing through the bound vector solitons, which indicates that the soliton and the bound solitons may strongly interact with each other when they overlap in the space. Our experimental result clearly shows that the collision destroys neither the bound state of the vector solitons nor the single vector soliton. Visualization 3 shows another situation experimentally observed. In the



situation a soliton bunch is initially in the laser cavity. A soliton bunch is different from a bound state of solitons in that the adjacent solitons are far apart from each other and loosely bound. However, the bunch as a unit propagates in the cavity. A soliton bunch propagates with a very different group velocity in the cavity from that of the single soliton, therefore, they collide in the cavity. Different from that shown in [Visualization 2](#) where the single soliton passes through the bound solitons, the soliton bunch shown in [Visualization 3](#) behaves like a soliton sink, which simply absorbs the solitons coming to it. It is worth mentioning that a similar phenomenon was reported theoretically where the interaction between a soliton and a multi-soliton array is modeled based on the CGLE [23, 24].

### 3.5 A bound state of bound vector solitons

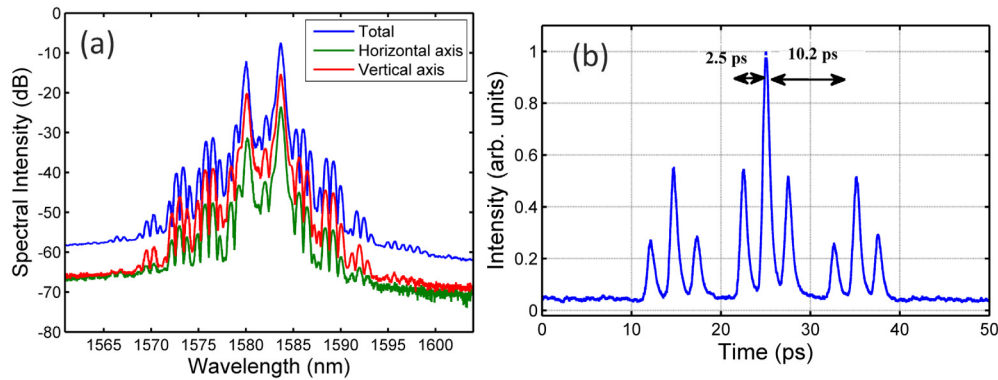


Fig. 6. A bound state of bound vector solitons. (a) Optical spectra; (b) Autocorrelation trace.

Like first experimentally observed in a soliton fiber laser mode locked with the NPR technique [7], bound states of bound vector solitons are also experimentally observed in the graphene mode locked fiber laser. A typical example is shown in Fig. 6. Here a bound state of bound vector solitons is referred to as the state where two sets of the bound vector solitons are very close to each other and bind together through the direct soliton interaction. Figure 6(a) is the polarization resolved optical spectra of the laser emission. The vector nature of the bound solitons is confirmed by the polarization resolved spectra. There are two sets of modulation in the spectra correspond to the vector soliton separations in primary bound solitons, which is about 2.5 ps, and the separation between the primary bound-solitons, which is about 10.2 ps. Figure 6(b) shows the measured autocorrelation trace. It clearly shows the pulse separations. The autocorrelation measured pulse separations are well in agreement with those calculated from the spectral modulation periods. We note that bound states of bound solitons were previously also observed in the carbon nanotube mode locked fiber lasers [9].

## 4. Discussion

The graphene mode locked fiber lasers have now been experimentally extensively investigated. Since polarization independent saturable absorption could be easily achieved with the graphene-based saturable absorbers, through exploiting the nonlinear light propagation in the vector cavity fiber lasers, one could easily achieve the vector soliton operation in the graphene mode locked fiber laser. Due to the dissipative nature of the formed solitons in a fiber laser, under strong pumping multiple vector solitons could further be formed. Multiple solitons in a fiber laser can have complicated interaction. Previous experimental studies based on multiple scalar solitons have shown various types of interaction forces, the global interaction caused by the continuous wave in the cavity, the dispersive waves mediated interaction and the direct soliton interaction. Our experimental results suggest that even for the vector solitons, these types of interactions still remain. Obviously the vector nature of the solitons does not change their interaction features. Moreover, the various



soliton interactions did not destroy the vector soliton either. This result shows that the polarization coupling strength is very strong. This could also be easily understood, as the polarization coupling could also be treated as a kind of direct solitons interaction.

As a result of different types of soliton interactions, as well as under different conditions, different situations of the multiple vector soliton operation have been observed in our fiber laser. What we have shown here are just some of the special cases, it is anticipated that more interesting cases could be further obtained. We hope that our results could trigger further extended studies.

## 5. Conclusion

In conclusion, we have experimentally investigated the vector soliton operation of a graphene mode locked fiber laser. It has been shown that under strong pumping, multiple vector solitons could be formed in the fiber laser, and as a result of the various types of the soliton interactions, different forms of stable and dynamic multi-vector-soliton operation states could be formed. These include the bound states of vector solitons, and bound states of the bound vector solitons. Coexistence and interaction of vector soliton and bound vector solitons is obtained and experimentally investigated. In addition, collision between the vector solitons is experimentally visualized. Our experimental results demonstrated the richness of the vector soliton interactions and the formed phenomena.

## Acknowledgments

This project is partially supported by the funds of Priority Academic Program Development of Jiangsu Higher Education Institutions (PAPD), China, and Minister of Education (grant no. 35/12), Singapore, and AOARD under Agreement No. FA2386-13-1-4096, and National Natural Science Foundation of China (NSFC) (61222505, 61435010, 61575089).